Exhibition of intrinsic properties of certain systems in response to external disturbances

P. S. Landa[1] and A. Rabinovitch[2]
[1]*Department of Physics, Lomonosov Moscow State University, 119899 Moscow, Russia*
[2]*Physics Department, Ben-Gurion University of the Negev, 84105 Beer-Sheva, Israel*
(Received 15 June 1999)

Two systems, which are models of biological processes, are considered. These systems are notable for responding to different external actions nearly alike. This is associated with the fact that an external action excites only their natural intrinsic motions. Two kinds of external actions, harmonic and random, are studied. It is shown that each of them induces a transition to a new state that can be treated as a peculiar kind of phase transitions. Characteristics of these phase transitions are found.

PACS number(s): 87.10.+e, 87.23.Cc, 87.19.La

I. INTRODUCTION

Usually, the response of a system to external disturbances of different kinds is different. For example, a harmonic external force applied to a simple nonlinear oscillator causes, as a rule, periodic oscillations, whereas a random force results in random oscillations. Even if chaotic oscillations result from a harmonic force, they, as a rule, differ essentially from random oscillations excited by noise.

However, as will be shown below, there exist systems which respond to different external disturbances in nearly the same manner, since there an external disturbance causes the system to reveal only its built-in character of motion, i.e., its intrinsic properties. We consider here two such systems, each being a model of a certain biological process. We think that the latter is not a coincidence, because biological systems are known to be robust with respect to the character of the disturbance. The first system is a standard model for childhood epidemics caused by seasonal variations of the contact rate. The second is a simple model for excitation of neural pulses.

II. RANDOM AND CHAOTIC OSCILLATIONS IN A STANDARD MODEL FOR CHILDHOOD EPIDEMICS CAUSED BY SEASONAL VARIATIONS OF THE CONTACT RATE OF SUSCEPTIBLE CHILDREN WITH INFECTIVE ONES

It is known that childhood diseases, such as chickenpox, measles, mumps, and rubella, vary seasonally in their extention [1,2]. A standard epidemiological model for the description of these variations, taking into account seasonal variations of the contact rate of children susceptible to infection with infective ones, includes four categories: (1) Susceptibles (S), (2) exposed but not yet infective (E), (3) infective (I), (4) recovered and immune (R). For this reason the model under consideration is often called SEIR. Mutual relations between these categories are illustrated schematically by Fig. 1. The relative number of children S susceptible to infection increases with the total number of children and decreases both owing to the fact that a portion of them remains unexposed and owing to a transfer of children from this category into the category of the exposed but not yet infective (E). A portion of the children exposed remains noninfective, whereas another portion goes over into the category of the infective ones (I). In its turn, a portion of the infective children does not fall sick while another portion, having had the disease, becomes recovered, and is transferred to the fourth category (R). Taking into account that the total number of children is constant, the equations for this model can be written as

$$\dot{S}=m(1-S)-bSI, \quad \dot{E}=bSI-(m+a)E,$$

$$\dot{I}=aE-(m+g)I, \tag{1}$$

$$\dot{R}=gI-mR, \tag{2}$$

where $1/m$ is the average expectancy time, $1/a$ is the average latency period, $1/g$ is the average infection period, b is the contact rate (the average number of susceptibles contacted yearly with infective). Let us note that Eqs. (1) do not contain the variable R; hence these equations can be considered independently of Eq. (2).

Equations (1) were first considered by Dietz [3]. Dietz assumed the periodic variation of the contact rate b with the period of one year and found analytically a periodic solution of the model equations. Later these equations were studied in detail by Olsen and Schaffer [4] and Engbert [5]. It was shown that periodic variations of the contact rate can result not only in periodic oscillations of childhood infections but in chaotic ones as well.

It is easily shown that for time-independent contact rate $b=\text{const}=b_0$ Eqs. (1) have, depending on the parameters, either one [for $ab_0 \leqslant (m+a)(m+g)$] or two [for $ab_0 > (m+a)(m+g)$] singular points: one of them with coordinates $S=1$, $E=I=0$ and the other one (if it exists) with coordinates

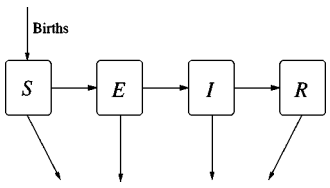

FIG. 1. Diagram illustrating mutual relations between different components in the SEIR model.

$$S_0=\frac{(m+a)(m+g)}{ab_0},\quad E_0=\frac{m}{m+a}-\frac{m(m+g)}{ab_0},$$
$$I_0=\frac{am}{(m+a)(m+g)}-\frac{m}{b_0}. \tag{3}$$

In the case when there is only one singular point it is stable, whereas in the case when both of the singular points exist the first of them is aperiodically unstable and the second is stable. These cases are said to correspond to extinction of epidemics and endemic equilibrium, respectively.

It is shown in Ref. [4] that the values of the model parameters most closely corresponding to the estimates made for childhood diseases in first world countries are $m=0.02\ \mathrm{y}^{-1}$, $a=35.84\ \mathrm{y}^{-1}$, $g=100\ \mathrm{y}^{-1}$, $b_0=1800\ \mathrm{y}^{-1}$. For these parameters Eqs. (1) have two singular points. In our studies we have used these values of the parameters.

If the parameter b oscillates with time then the variables S, E, and I oscillate too, and these oscillations are executed about the stable singular point with the coordinates (3). Therefore, it is convenient to substitute into Eqs. (1) the new variables $x=S/S_0-1$, $y=E/E_0-1$, and $z=I/I_0-1$. Putting $b=b_0[1+b_1f(t)]$, where $f(t)$ is a function describing the shape of the contact rate oscillation, let us rewrite Eqs. (1) in the variables x, y, z:

$$\dot{x}+mx=-b_0I_0\{[1+b_1f(t)](x+z+xz)+b_1f(t)\},$$
$$\dot{y}+(m+a)y=(m+a)\{[1+b_1f(t)](x+z+xz)+b_1f(t)\}, \tag{4}$$
$$\dot{z}+(m+g)z=(m+g)y.$$

In Eqs. (4) the term $b_1f(t)$ can be considered as an external action upon the system. We see from Eq. (4) that this action is not only multiplicative, i.e., parametric, but also additive, i.e., forcing. It should be noted that owing to quadratic nonlinearity the forcing action, even when not in resonance, can cause a strong response of the system.

For $b_1=0$ and small initial deviations from the equilibrium state $x=0$, $y=0$, $z=0$ the system executes damped oscillations which are close to harmonic ones in shape [Fig. 2(a)]. The frequency of these oscillations $\omega_0\approx\pi$. As the initial deviations increase, the natural oscillations of the system become close to disconnected, as exemplified by Fig. 2(b). The frequency of the natural oscillations decreases as their amplitude increases.

A. Periodic oscillations of the contact rate

As mentioned above, in Refs. [3,4] it was assumed that owing to seasonal variations of environmental conditions the contact rate b depends periodically on time with a period of one year, viz., $f(t)=\cos\omega t$, where $\omega=2\pi$. We emphasize that this frequency is approximately equal to the doubled natural frequency of small free oscillations of the model variables, ω_0.

It was shown that the periodic variation of the parameter b causes the appearance of either periodic or chaotic oscillations of the variables S, E, and I. For very small b_1 the oscillations excited are close to harmonic ones with the frequency of the action ω [Fig. 3(a)]. For a certain value of b_1

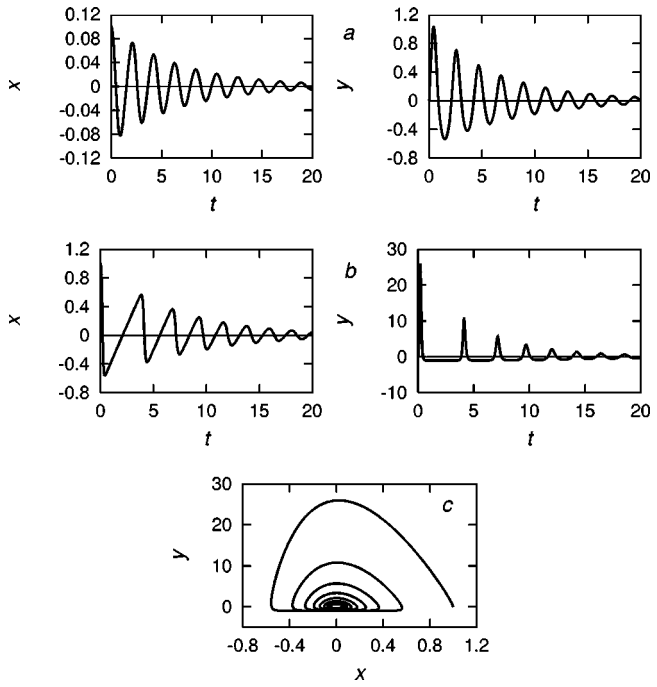

FIG. 2. Natural oscillations of the SEIR model variables x and y for $y(0)=0$, $z(0)=0$, $x(0)=0.1$ (a) and $x(0)=1$ (b); (c) the phase portrait. The values of the parameters are determined by Eq. (4). The shape of the variable z is similar to that of y.

a period-doubling bifurcation occurs that is associated with a parametric mechanism of the oscillation excitation. As b_1 increases the main frequency of the oscillations remains equal to $\omega/2$ while the shape of the oscillations of the variable x becomes close to saw-tooth [Fig. 3(b)]. On further increasing b_1 another period-doubling bifurcation takes place

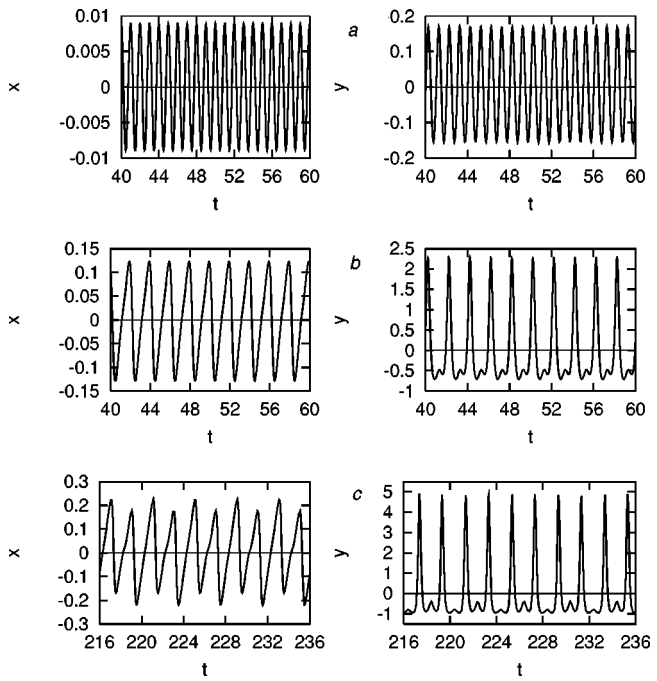

FIG. 3. The time dependencies of the SEIR model variables x and y in the case of the periodic variation of the contact rate for $b_1=0.03$ (a), $b_1=0.1$ (b), and $b_1=0.26$ (c).

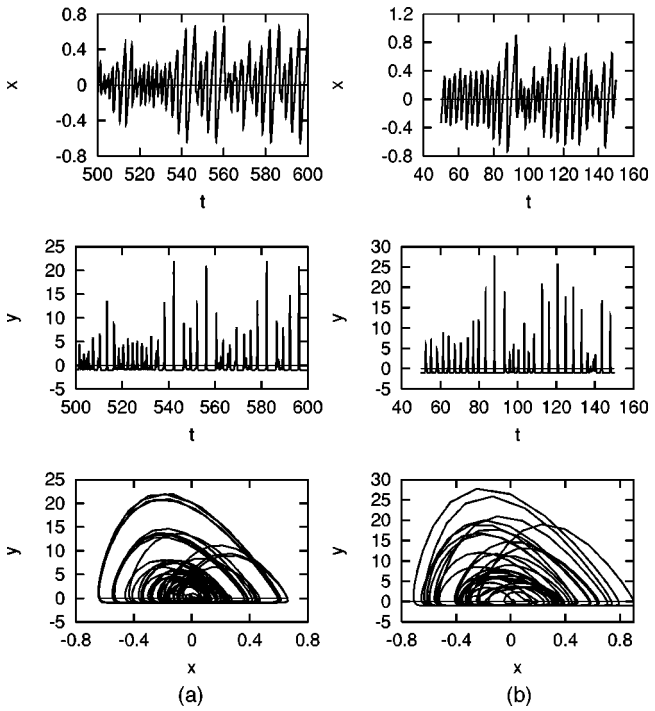

FIG. 4. The time dependencies of the SEIR model variables x and y, and the projection of the phase trajectory on the x,y-plane for $f(t)=\cos 2\pi t$, $b_1=0.28$ (a) and $f(t)=\chi(t)$, $b_1=0.235$ (b).

[Fig. 3(c)] and then a drastic transition to chaos, accompanied by a drastic increase in oscillation variance, occurs. We note that chaotic oscillations for $b_1=0.28$ were first found numerically by Olsen and Schaffer [4]. For this value of b_1 the time dependencies of x and y, and the projection of the phase trajectory on the x, y plane found by numerical simulation of Eqs. (4) are shown in Fig. 4(a). It should be noted that these oscillations in their form closely resemble the experimental data. This fact seemingly justifies the model with a periodic variation of the contact rate. However, as it is seen from Fig. 4(b), similar results can also be obtained for a random variation of the contact rate. The similarity between the shapes of the oscillations is associated with the fact that the variation of the contact rate only induces a transition to an oscillatory state (see below) whereas the shape of the induced oscillations is mainly determined by the intrinsic properties of the system, which also manifest themselves in the shape of its free oscillations.

The evolution of the power spectra of the oscillations in the case of a periodic variation of the contact rate is illustrated in Fig. 5. We see that for $b_1=0.03$ the spectral density does peak at the frequency ω, whereas for $b_1=0.1$ it peaks at the frequency $\omega/2$. For $b_1=0.26$ the power spectrum contains the forth subharmonic, and for $b_1=0.28$, when the oscillations are chaotic, the spectrum becomes continuous with a maximum at the frequency $\omega/4$.

The excitation of the oscillations at the frequency $\omega/2=\pi$ can be considered as a phase transition induced by the periodic variation of the contact rate. This consideration is supported by the dependence of the variance of the variable x, which we denote by σ^2, on the parameter b_1 [Fig. 6(a)]. We see that for b_1 close to $b_1^{(cr)}\approx 0.066$ the rate of change of the variance increases drastically. The dependence of σ^2 on

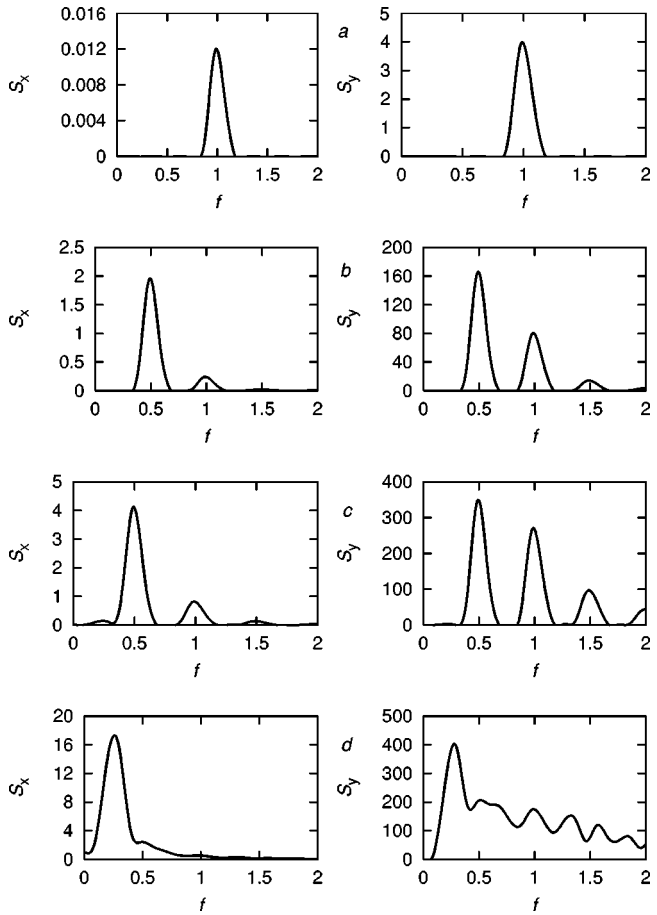

FIG. 5. The evolution of the power spectra for $x(t)$ and $y(t)$ in the case of harmonic variation of the contact rate: $b_1=0.03$ (a), $b_1=0.1$ (b), $b_1=0.26$ (c), and $b_1=0.28$ (d). We see that the spectra for $y(t)$ are wider than those for $x(t)$.

b_1 can be approximated by the formula $\sigma^2=0.038(b_1-b_1^{(cr)})^{1/2}$. Such a dependence is typical of the second order phase transitions, if one considers σ^2 as an analog of the order parameter and b_1 as an analog of the temperature. In this approach the critical index is equal to 1/2. For $b_1\approx 0.27$ another transition occurs, revealing itself in a transition from periodic oscillations to chaotic ones and in a jumplike increase of the variance [Fig. 6(b)]. This transition can be considered as an induced phase transition of the first kind.

To clarify the physical mechanisms of the phase transitions let us change somewhat Eqs. (4) so that the amplitudes of the parametric and the forcing actions could be varied independently. Namely, let us rewrite Eqs. (4) as

$$\begin{aligned}\dot{x}+mx&=-b_0I_0\{[1+b_1f(t)](x+z+xz)+b_2f(t)\},\\ \dot{y}+(m+a)y&=(m+a)\{[1+b_1f(t)](x+z+xz)+b_2f(t)\},\\ \dot{z}+(m+g)z&=(m+g)y.\end{aligned}\tag{5}$$

First we consider the case when the additive action is absent, i.e., $b_2=0$, $b_1\neq 0$. In this case the dependence of σ^2 on b_1 is shown in Fig. 7(a). It is seen that oscillations are excited only from a certain critical value of the parameter b_1 onward. This is the characteristic property of parametric ex-

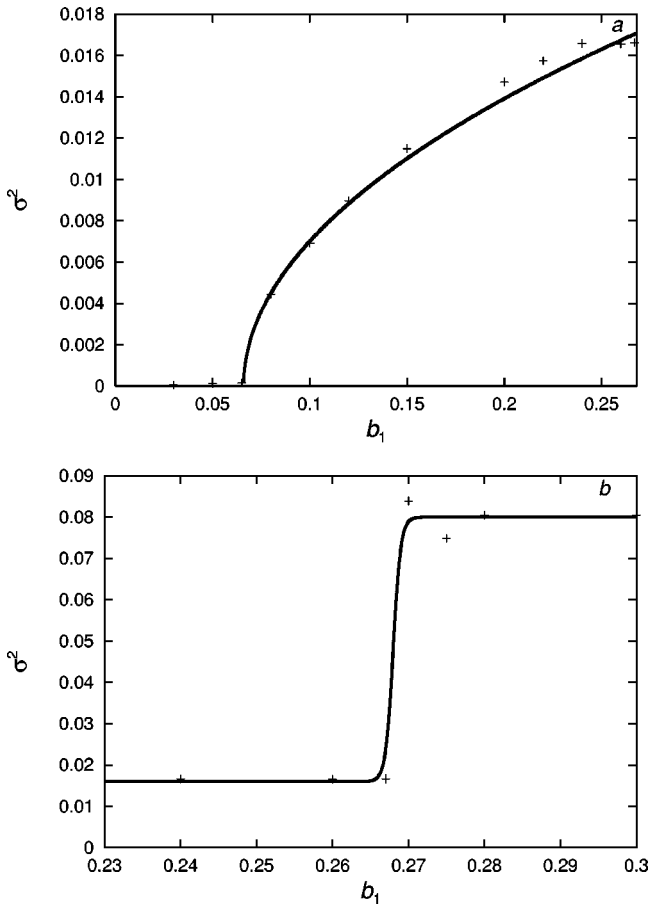

FIG. 6. The plot of the variance of the variable x (σ^2) in the SEIR model versus the parameter b_1 in the range $0 \leqslant b_1 \leqslant 0.268$ (a) and in the range $0.23 \leqslant b_1 \leqslant 0.3$ (b). The dependence $\sigma^2 = 0.038(b_1 - 0.066)^{1/2}$ is shown in (a) as a solid line.

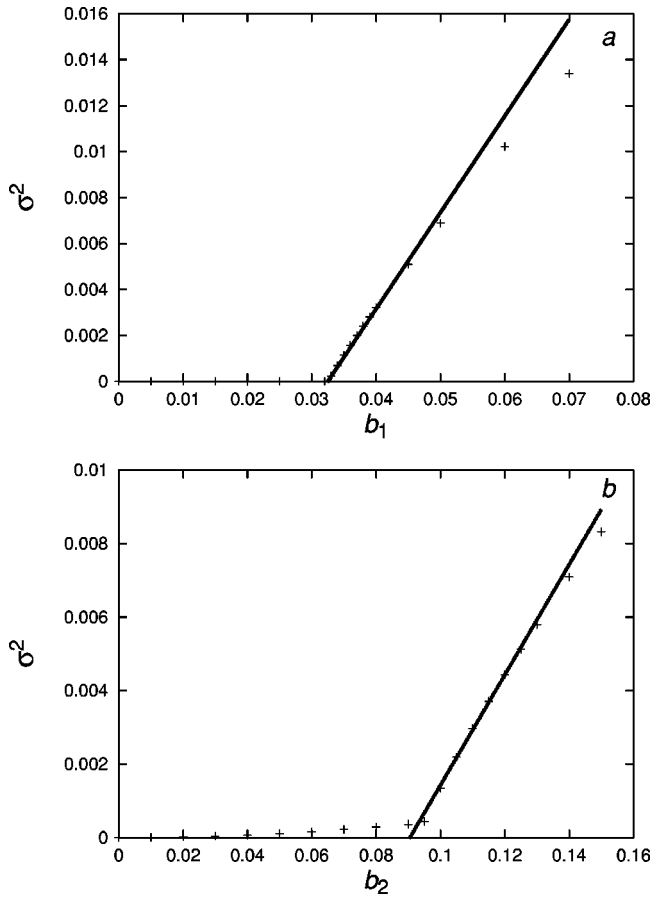

FIG. 7. The plot of σ^2 versus the action amplitude for parametric (a) and forcing excitation of oscillations of the SEIR model; the dependencies $\sigma^2 = 0.42(b_1 - 0.0325)$ (a) and $\sigma^2 = 0.15(b_2 - 0.0905)$ (b) are shown as solid lines.

citation of oscillations (see, for example, Ref. [6]). As the difference between b_1 and its critical value $b_1^{(cr)} \approx 0.0325$ increases, the variance increases nearly linearly. The critical index for this case is therefore 1. For $b_1 > 0.75$ the solution becomes unstable and goes to infinity.

In the case when the action is only additive, i.e. $b_1 = 0$, $b_2 \neq 0$ oscillations are excited even for values of b_2 as small as is wished. However, for $b_2 < b_2^{(cr)}$, where $b_2^{(cr)} \approx 0.0885$, the amplitude of these oscillations is very small and their frequency is equal to ω. For $b_2 \approx b_2^{(cr)}$ the rate of change of the variance of the oscillations increases rapidly and for $b_2 > b_2^{(cr)}$ the dependence of σ^2 on b_2 can be approximated by the straight line $\sigma^2 = 0.14(b_2 - b_2^{(cr)})$ [see Fig. 7(b)]. The drastic increase in the rate of change of the variance is associated with the appearance of subharmonic resonance. And indeed, the main frequency of the oscillations excited, for $b_2 > b_2^{(cr)}$, becomes equal to $\omega/2$. Considering this process as a second order phase transition, we can conclude that, in the case of only additive action, as for only parametric action, the critical index is equal to 1. For $b_2 > 0.15$ the solution, as in the case of parametric excitation, becomes unstable and goes to infinity. The computation of Eqs. (5) shows that the combined effect of parametric and forcing actions, which was described above, results in the stabilization of the solution for moderately large amplitudes.

B. Random oscillations of the contact rate

From a physical standpoint a random variation of the contact rate is more justified than periodic one. It is evident that $b(t)$ has to be a sufficiently wide-band random process for which the spectral density peaks at the frequency corresponding to a period of one year. Starting from this assumption we have numerically simulated Eqs. (4) with $f(t) = \chi(t)$, where $\chi(t)$ is a random process which is a solution of the equation

$$\ddot{\chi} + 2\pi\dot{\chi} + 6\pi^2\chi = k\xi(t), \tag{6}$$

$\xi(t)$ is white noise, k is the factor which is chosen so that the variance of $\chi(t)$ would be 1/2. The plots of $\chi(t)$ and of its spectral density are shown in Fig. 8.

The results of the numerical simulation of Eqs. (4) with $f(t) = \chi(t)$ are shown in Fig. 4(b) for the same values of the parameters as in Fig. 4(a) but for $b_1 = 0.235$. The latter was chosen so that the variance of $x(t)$ would be approximately the same as for $f(t) = \cos 2\pi t$, $b_1 = 0.28$. It is seen from this figure that the noise-induced oscillations differ very slightly in their form both from those for the case of harmonic variation of the contact rate and from the experimental data. The power spectra of the oscillations induced by the random and by the harmonic variation of the contact rate are also similar: both of them peak at the frequency $\omega/4$ [compare Figs. 5(d)

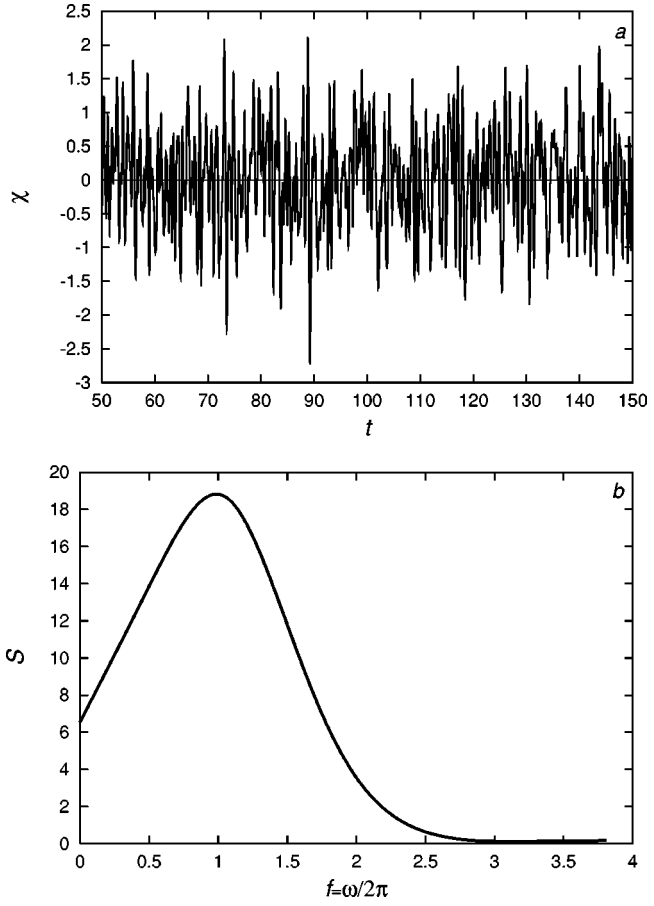

FIG. 8. The plots of $\chi(t)$ and its spectral density. We see that the spectral density of $\chi(t)$ peaks at the frequency 2π.

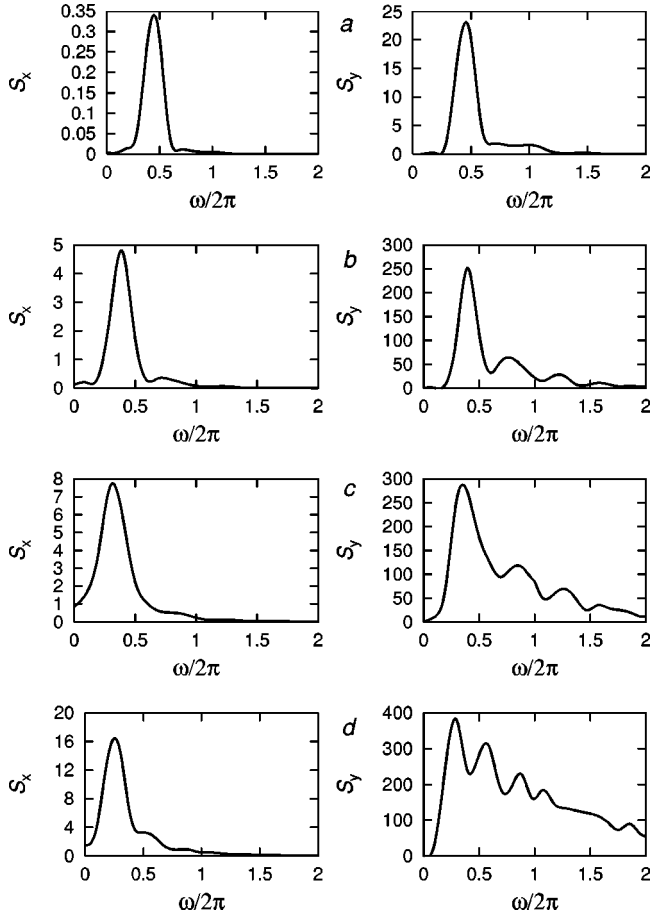

FIG. 9. The evolution of the power spectra for the SEIR model variables $x(t)$ (left column) and $y(t)$ (right column) in the case of random variation of the contact rate: $b_1=0.03$ (a), $b_1=0.1$ (b), $b_1=0.2$ (c), and $b_1=0.235$ (d). We see that, as for the case of periodic variation of the contact rate, the spectra for $y(t)$ are wider than those for $x(t)$.

and 9(d)]. It should be noted that in the case of random variation of the contact rate the power spectrum is always continuous (see Fig. 9); as b_1 increases the maximum of the spectrum shifts to lower frequencies.

Similar to the harmonic variation of the contact rate, the random variation also induces a transition similar to a phase transition [7]; in this process the multiplicative component of the random action induces a phase transition much as for a pendulum with randomly vibrated suspension axis [8,9]; whereas the additive component induces a transition much as for a nonlinear oscillator with quadratic nonlinearity [6]. The joint action of both components results in the dependence of the variance of $x(t)$ on b_1 shown in Fig. 10. In a certain range of b_1 this dependence can be approximated by a straight line. The value of b_1 for which this straight line intersects the abscissa is equal to 0.066, i.e., it is the same as that for the harmonic variation of the contact rate. However in this case the critical index is equal to 1 but not to 1/2.

To study the transitions in question in more detail we have attempted to simulate Eqs. (5), (6) with $f(t)=\chi(t)$ and put $b_2=0$, $b_1\neq 0$ and *vice versa*. It is found that in the case of only multiplicative action the transition occurs via on-off intermittency as for a pendulum with randomly vibrated suspension axis [10,11]. The critical value of the parameter b_1 is approximately equal to 0.095, i.e., essentially larger than in the case of harmonic variation of the contact rate. An example of oscillations of the variables x and y for $b_1=0.099$, illustrating the on-off intermittency, is given in Fig. 11. Un-

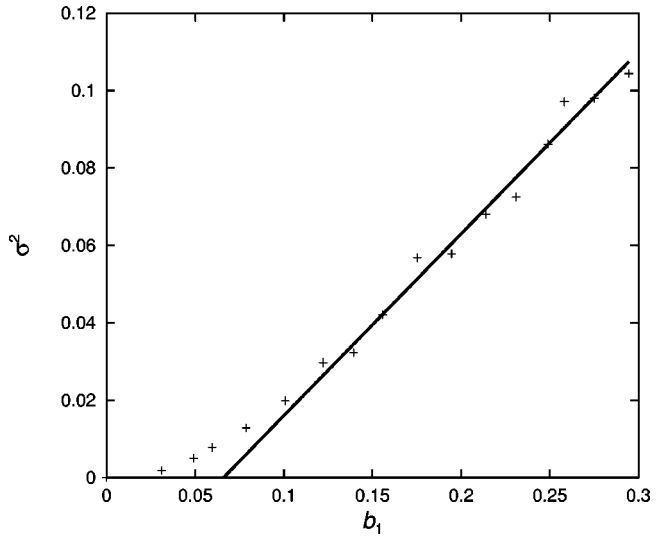

FIG. 10. The dependence of the variance of $x(t)$ on the parameter b_1 in the case of random variation of the contact rate in the SEIR model. The solid line shows the straight $\sigma^2=0.47(b_1-0.066)$.

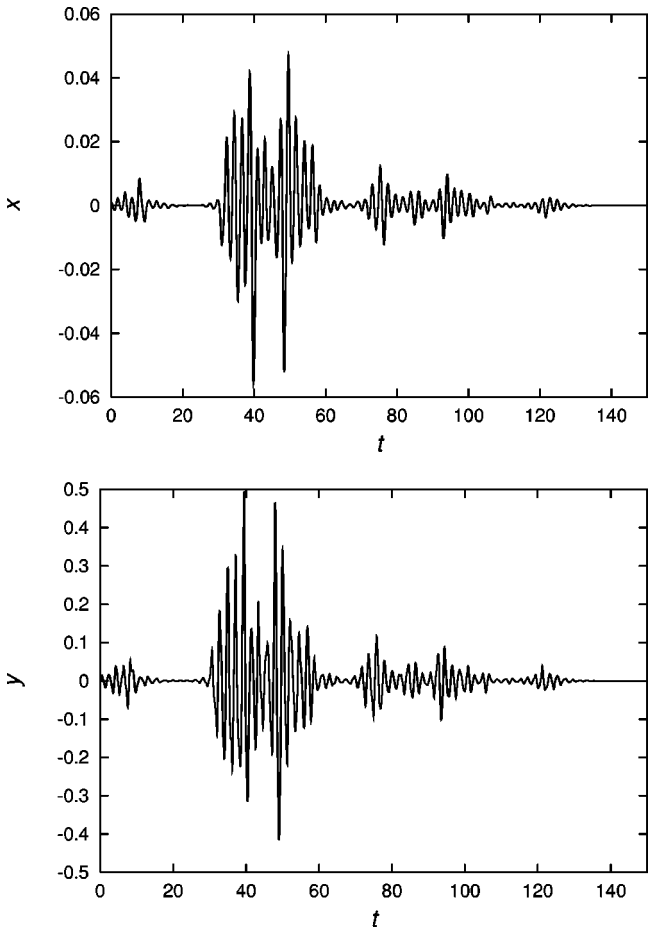

FIG. 11. An example of oscillations of the SEIR model variables x and y for $b_1=0.099$ in the case of only multiplicative random action.

fortunately, it appears to be impossible to find the characteristics of the transition, i.e., the dependence of the oscillation variance on b_1, because even for $b_1=0.1$ the solution goes to infinity. In the case when $b_1=0$, $b_2\neq 0$, the system behaves in a similar manner: the solution goes to infinity for $b_2 \geqslant 0.08$.

III. BONHOEFFER–van der POL OSCILLATOR

The equations of a so-called Bonhoeffer–van der Pol oscillator were suggested by Bonhoeffer for simulating neural pulses [12–15]. They are a generalization of the van der Pol equations for relaxation oscillations [16]. These equations describe oscillations of the voltage x across a neural membrane with consideration of the refractoriness characterized by the variable y. Later similar equations, incorporating spatial diffusion, came to be known as FitzHugh–Nagumo equations [17–19]. The Bonhoeffer–van der Pol equations can be written as [20]

$$\dot{x}=x-\frac{x^3}{3}-y+I(t), \quad \dot{y}=c(x+a-by), \tag{7}$$

where a, b, and c are the membrane radius, the specific resistivity of the fluid inside the membrane, and the temperature factor, respectively; $I(t)=I_0+F(t)$ is the current across the membrane with I_0 being the direct component of this current.

For $F(t)=0$ and the parameters corresponding to real membranes (following, for example, Ref. [21] we set $a=0.7$, $b=0.8$, and $c=0.1$) Eqs. (7) have a single singular point $x=x_0$, $y=y_0=(x+a)/b$, where x_0 is a real root of the equation

$$\frac{x^3}{3}+\left(\frac{1}{b}-1\right)x+\frac{a}{b}-I_0=0. \tag{8}$$

In the ranges $I_0<0.341$ and $I_0>1.397$ this point is a stable focus; whereas for $0.341<I_0<1.397$ it is an unstable focus.

Setting $\xi=x-x_0$, $\eta=y-y_0$ we obtain for ξ and η the following equations:

$$\dot{\xi}=-\left(\frac{\xi^3}{3}+x_0\xi^2+(x_0^2-1)\xi+\eta\right)+F(t),$$
$$\dot{\eta}=c(\xi-b\eta). \tag{9}$$

The case when the system under consideration is not self-oscillatory is of prime interest for the purpose of this paper. Therefore we restrict our consideration to the case of $I_0=0.2$. Eqs. (9) are notable for that they have two exceptional phase trajectories [22]. One of these trajectories has a positive Lyapunov exponent, i.e., it is unstable, whereas the other is stable. The first has a part which repels all neighboring phase trajectories, while the second has two parts which attract all neighboring phase trajectories. Evidently, these exceptional trajectories are not a repeller and an attractor in the strict sense, since the system described by Eqs. (9) for $I_0=0.2$ has no repellers and only a single attractor: the stable singular point. However, due to some similarity of these trajectories to repeller and attractor, in Ref. [23] they were called transient repeller and transient attractor, respectively. We will follow these names. It should be noted that there is variability in names of these trajectories. For example, in Ref. [24] they are called local separatrices and local attractors, in Ref. [25] the attracting trajectory is called phantom attractor and so on.

To find numerically the transient repeller, we can reverse the direction of time. As a result, we obtain the picture on the phase plane shown in Fig. 12(a). The part which repels all neighboring phase trajectories is shown as a thick solid line. A full phase portrait involving both the transient repeller and transient attractor is given in Fig. 12(b). The attracting parts are shown as thick solid lines. We see that the transient repeller separates the regions of deviations from the equilibrium state corresponding to radically different transient processes.

If the current $I(t)$ across the membrane contains an alternating component, for example, $F(t)=A\cos\omega t$, then, from a certain critical value of A onward, oscillations associated with the motion of the representative point along a phase trajectory involving the attracting parts are excited [26,27]. It follows from the results of numerical simulations of Eqs. (9) that the oscillation amplitudes of the variables ξ and η increase nearly by jump in this process [compare Figs. 13(a) and 13(b)]. The excitation of such oscillations, accompanied

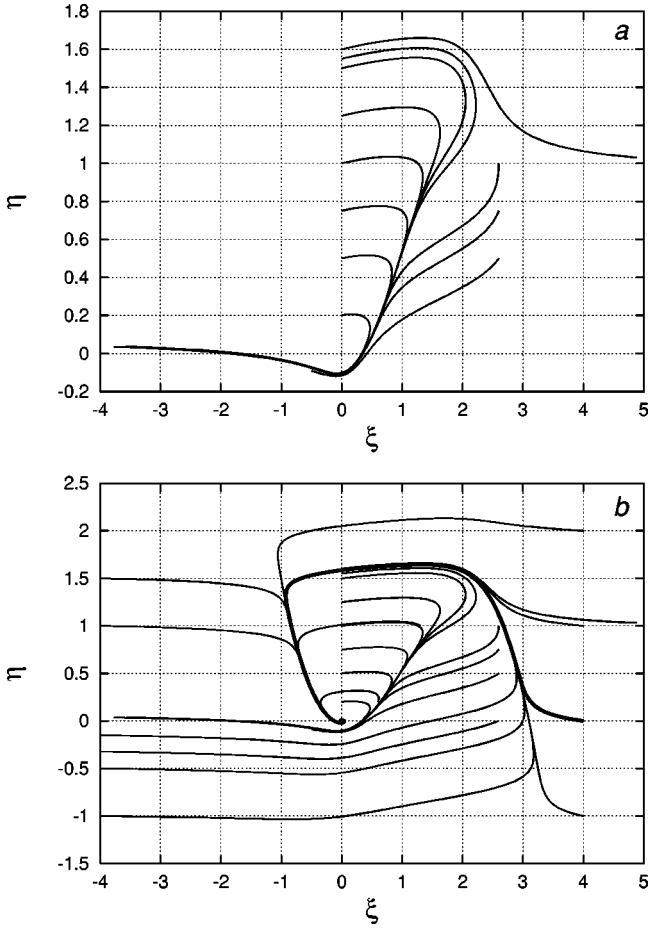

FIG. 12. The transient repeller and neighboring phase trajectories for the Bonhoeffer–van der Pol oscillator (a), and the phase portrait involving the transient repeller and transient attractors (b) for $a=0.7$, $b=0.8$, $c=0.1$, and $I_0=0.2$.

by a drastic increase in the oscillation variance, can be considered as a phase transition. An example of the dependence of the variance of the variable $\xi(t)$ on A for $\omega=0.3$ is given in Fig. 14(a). We can conclude from this figure that the phase transition caused by the harmonic component of the current across the membrane is of the first kind (rather than of the second one). It is interesting that the jump has a fine structure: there are local ups and downs in the variance growth [Figs. 14(b) and 14(c)]. This fine structure is associated with drastic changes in the oscillation's shape under small changes of A (see Figs. 13 and 15).

The critical value of A depends on the frequency ω; it is minimal for a certain value of the frequency which in turn depends on I_0 [27]. The reason for this dependence is the resonance response of a nonlinear oscillator to a harmonic external force. As an example, the dependence of the critical value of the amplitude A on the frequency ω is shown in Fig. 16 for $I_0=0.2$. We see that the critical value of the amplitude is minimal for $\omega=0.27$, which is close to the frequency of small free oscillations about the equilibrium state equal to $\omega_0\approx 0.3146$.

For other values of the frequency the phase transition with increasing A occurs in a similar manner. This is illustrated by Fig. 17, where the dependencies of the variance of ξ on the amplitude A for $\omega=0.2$ and $\omega=0.4$ are given.

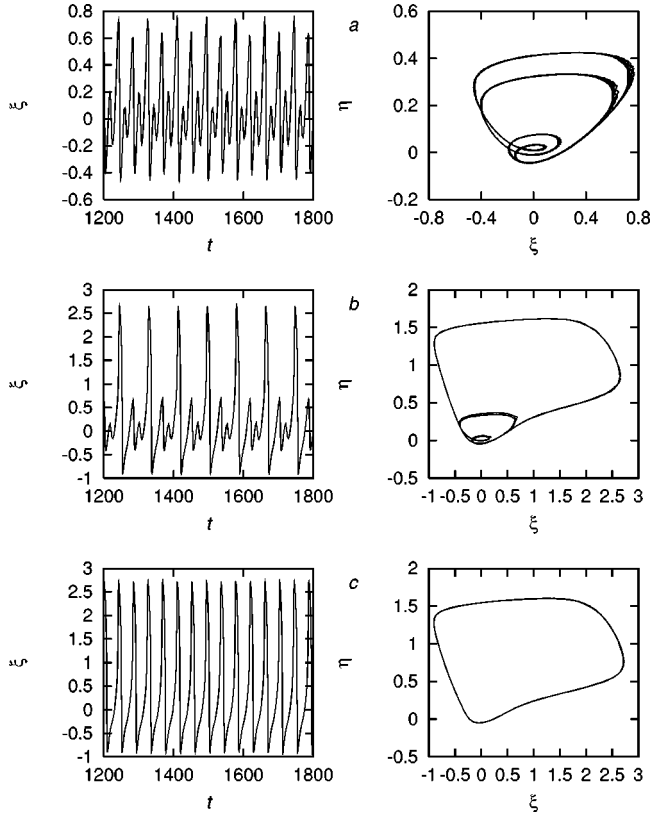

FIG. 13. Plot of $\xi(t)$ and the corresponding phase portraits for $\omega=0.3$, $A=0.057$ (a), $A=0.058$ (b), and $A=0.059$ (c).

If the alternating component of the current across the membrane $F(t)$ is a random process, for example white noise, then the transition to a new state is also observed, but it is of a radically different character. The appearance of a

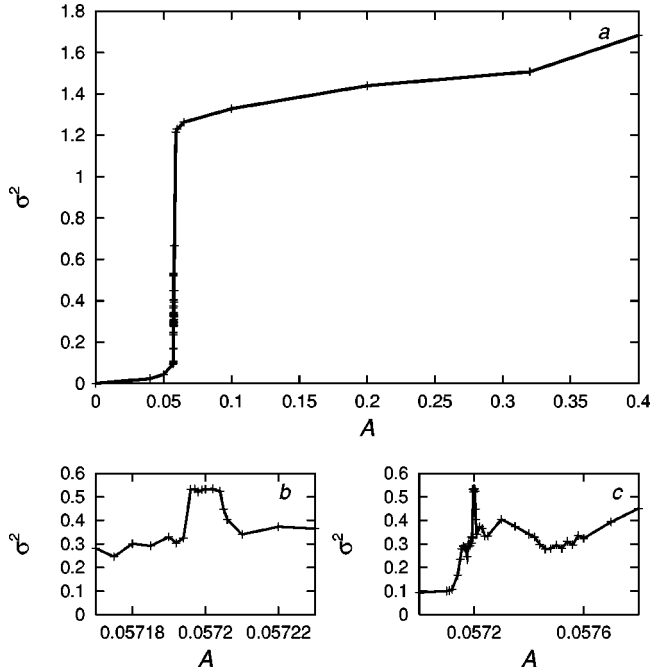

FIG. 14. The dependence of the variance of the variable ξ on the alternating current constituent amplitude A in the Bonhoeffer–van der Pol system for $\omega=0.3$ in the ranges $0\leqslant A\leqslant 0.4$ (a), $0.05717\leqslant A\leqslant 0.05723$ (b), and $0.0571\leqslant A\leqslant 0.0578$ (c).

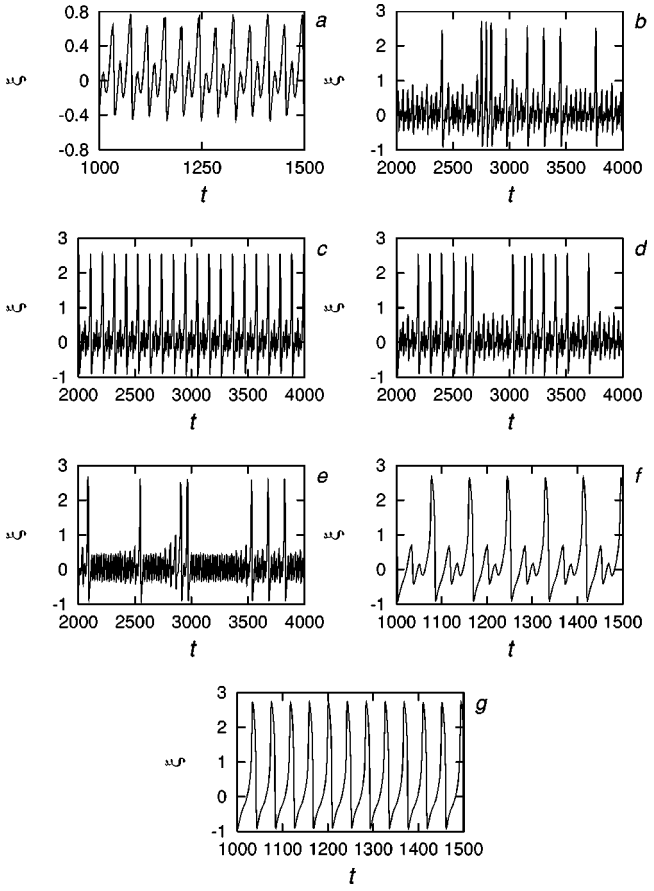

FIG. 15. The evolution of the time dependencies $\xi(t)$ for $\omega=0.3$ and $A=0.057$ (a); $A=0.05717$ (b); $A=0.0572$ (c); $A=0.05723$ (d); $A=0.05746$ (e); $A=0.058$ (f); and $A=0.059$ (g).

''limit cycle'' induced by white noise was considered in Refs. [24,28–30]. However, these works are mainly devoted to the calculation of the probability distributions in the vicinity of the induced ''limit cycle.'' We consider this phenomenon from the standpoint of the exhibition of the intrinsic properties of the system and the noise-induced transition to a new state. The latter is associated with the intersection of a boundary on the phase plane (the transient repeller is such a boundary) by the representative point under the action of noise. In principle, such intersection is possible for the noise intensity κ as small as is wished. Therefore the transition should occur smoothly as κ increases. Hence, in the strict sense this transition is not a phase transition. However, it is closely similar to a noise-induced second order phase transition. For example, the dependence of the variance of the variable ξ on the noise intensity κ, found by numerical simulation of Eqs. (9) and shown in Fig. 18(a), can be approximated on a certain interval by the formula $\sigma^2 \approx 5(\kappa - 0.0065)^{1/2}$. This formula is similar to that which describes the dependence of an order parameter on temperature for ordinary second order phase transitions with critical index equal to 1/2. Furthermore, it can be seen (see, e.g., Fig. 19) that this transition occurs via a peculiar kind of on-off intermittency. As for ordinary on-off intermittency [31,32,10,11], close to the transition onset the representative point in the phase plane is walking in a certain ϵ-vicinity of the equilibrium state over prolonged periods (so called ''laminar phases''), and only occasionally escapes from this vicinity. Contrary to ordinary on-off intermittency, these escapes have not a random but the strictly specified shape of pulses, and the duration of each of them is unchanged as the noise in-

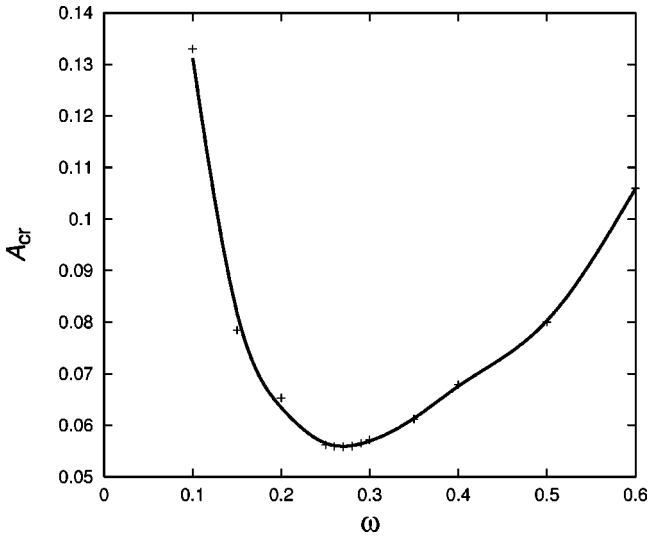

FIG. 16. The dependence of the critical value of the current alternating constituent amplitude A_{cr} on the frequency ω. The character of this dependence is caused by the resonance response of any nonlinear oscillator, including the Bonhoeffer–van der Pol one, to a harmonic external force.

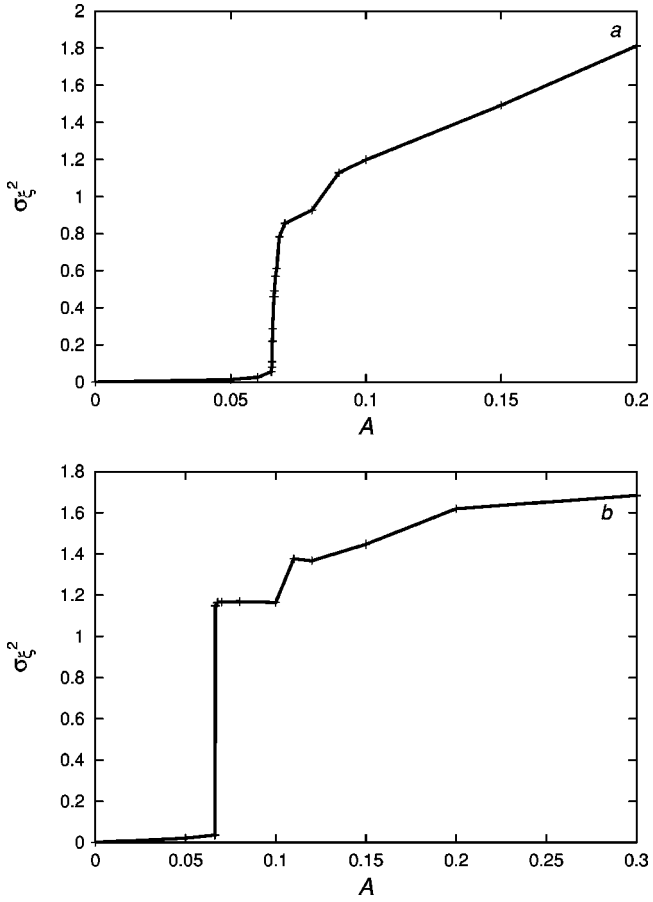

FIG. 17. The dependencies of the variance of the variable ξ on the current alternating constituent amplitude A for $\omega=0.2$ (a) and $\omega=0.4$ (b).

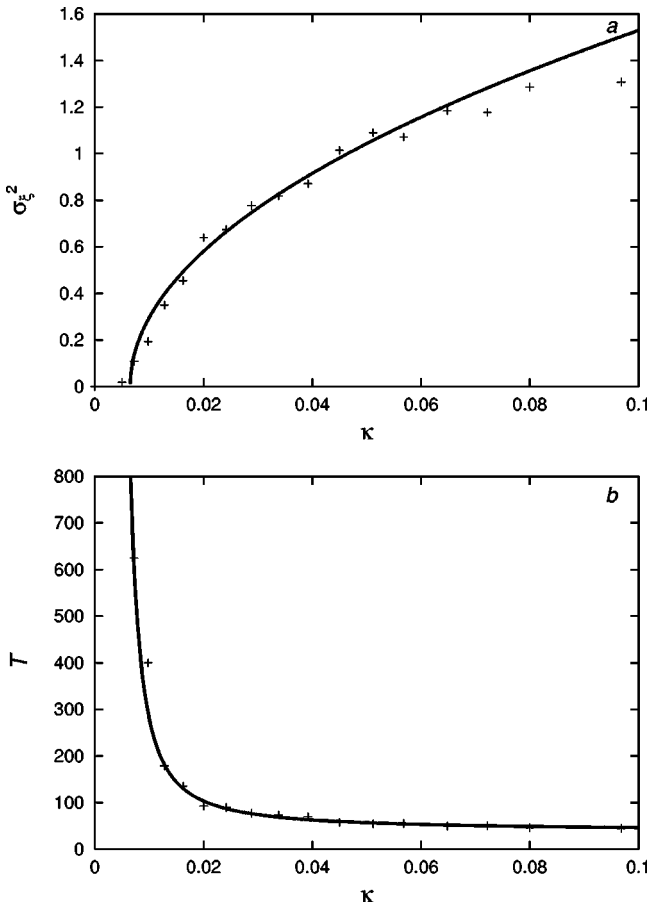

FIG. 18. The dependencies of the variance of the variable ξ (a) and the mean period T (b) on the noise intensity κ in the case when the alternating component of the current across the membrane $F(t)$ is white noise. Solid lines show the plots $\sigma_\xi^2 = 5\sqrt{\kappa - 0.0065}$ (a), and $T = 38\exp(0.02/\kappa)$ (b).

tensity increases. That is why these escapes should not be called ''turbulent phases.'' Away from the point of onset the duration of the laminar phases decreases and the variance of the system variables increases. Because here the duration of

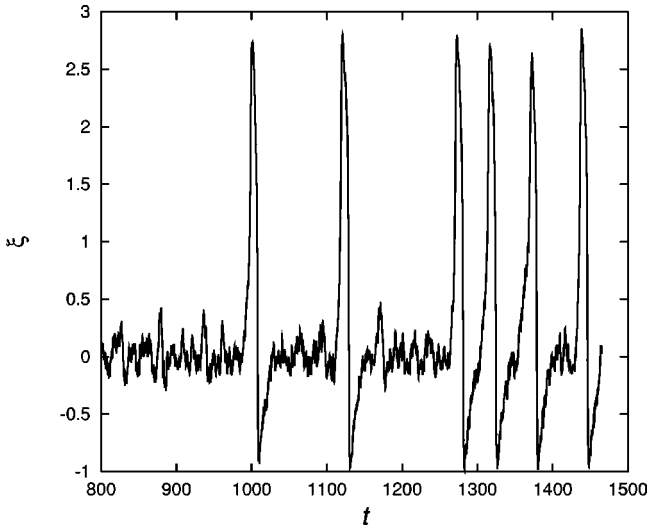

FIG. 19. An example of oscillations of the variable $\xi(t)$ for $\kappa = 0.0098$ demonstrating a peculiar kind of on-off intermittency close to the onset of the phase transition.

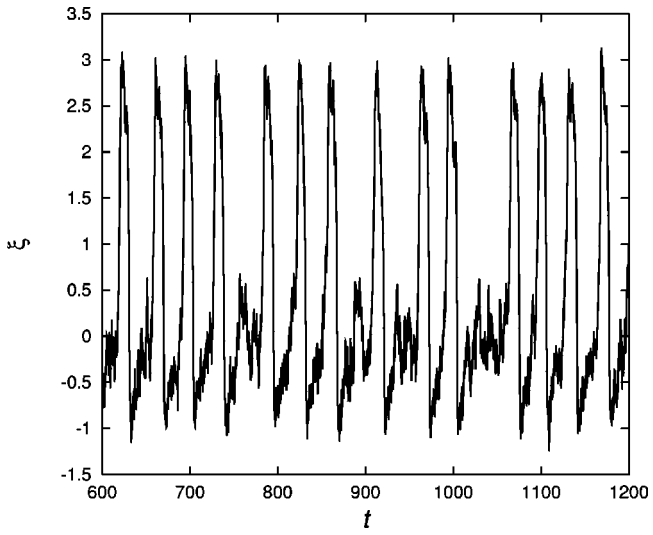

FIG. 20. Oscillations of the variable $\xi(t)$, induced by white noise, for $\kappa = 0.1152$.

the pulses is unchanged we can use the mean interpulse time (the mean period) in place of the mean duration of ''laminar phases.'' The dependence of the mean period T on the noise intensity κ is shown in Fig. 18(b). It can be approximated by the formula

$$T \approx 38 \exp\left(\frac{0.02}{\kappa}\right),$$

which is typical for a mean time of an intersection of a boundary [33,34]. We see that the mean period decreases exponentially as the noise intensity increases, that qualitatively agrees with the initial part of the corresponding dependence obtained in Refs. [24,28]. However, we have not found the increase of the mean period with increasing the noise intensity which is mentioned in this paper.

It should be noted that the pulses induced by noise differ little in shape from the pulses induced by a periodic force [compare Figs. 20 and 15(g)], with the only difference that the pulses induced by noise are somewhat noisy and the interpulse time is random. Intrinsic properties of the system reveal themselves in this similarity.

IV. CONCLUSIONS

In conclusion we note that the considered noise-induced phase transitions take place in a similar fashion to the phase transitions induced by a periodic action upon the same systems. In the SEIR model the difference between the noise-induced phase transitions and the transitions induced by a periodic action is only in the critical index. In the Bonhoeffer–van der Pol oscillator the transition induced by noise is actually not a phase transition but it is very similar to a second order phase transition, whereas phase transitions induced by a periodic force at a specific frequency are of the first order. The shape of the oscillations excited in consequence of these transitions is determined by the intrinsic properties of the systems and depends only slightly on the exciting action.

[1] W.P. London and J.A. Yorke, Am. J. Epidemiol. **98**, 453 (1973).
[2] L.F. Olsen and H. Degn, Q. Rev. Biophys. **18**, 165 (1985).
[3] K. Dietz, Lect. Notes Biomath. **11**, 1 (1976).
[4] L.F. Olsen and W.M. Schaffer, Science **249**, 499 (1990).
[5] R. Engbert and F.R. Drepper, Chaos Solitons Fractals **4**, 1147 (1994).
[6] P.S. Landa, *Nonlinear Oscillations and Waves in Dynamical Systems* (Kluwer Academic, Dordrecht, 1996).
[7] P.S. Landa and A.A. Zaikin, in *Applied Nonlinear Dynamics and Stochastic Systems Near the Millennium* (AIP Conf. Proc. 411) (AIP, New York, 1997), p. 321.
[8] P.S. Landa and A.A. Zaikin, Phys. Rev. E **54**, 3535 (1996).
[9] P.S. Landa and A.A. Zaikin, JETP **84**, 197 (1997).
[10] P.S. Landa and A.A. Zaikin, Chaos Solitons Fractals **9**, 157 (1998).
[11] P.S. Landa, A.A. Zaikin, M.G. Rosenblum, and J. Kurths, Phys. Rev. E **56**, 1465 (1997).
[12] K.F. Bonhoeffer, Z. Elektrochem. **47**, 147 (1941).
[13] K.F. Bonhoeffer, J. Gen. Physiol. **32**, 69 (1948).
[14] K.F. Bonhoeffer and G. Langhammer, Z. Elektrochem. **52**, 67 (1948).
[15] K.F. Bonhoeffer, Naturwissenschaften **40**, 301 (1953).
[16] B. van der Pol, Philos. Mag. **2**, 978 (1926).
[17] R. FitzHugh, Biophys. J. **1**, 445 (1961).
[18] J. Nagumo, S. Arimoto, and S. Yoshizawa, Proc. IRE **50**, 2061 (1962).
[19] R. FitzHugh, in *Biological Engineering*, edited by by H.P. Schwan (McGraw-Hill, New York, 1969), p. 1.
[20] M. Okuda, Prog. Theor. Phys. **66**, 90 (1981).
[21] S. Rajasekar and M. Lakshmanan, Physica D **32**, 146 (1988).
[22] A. Rabinovitch, R. Thieberger, and M. Friedman, Phys. Rev. E **50**, 1572 (1994).
[23] A. Rabinovitch and I. Rogachevskii, Chaos (to be published).
[24] H. Treutlein and K. Schulten, Ber. Bunsenges. Phys. Chem. **89**, 710 (1985).
[25] W.P. Wang, Nonlinearity **9**, 739 (1996).
[26] S. Yasin, M. Friedman, S. Goshen, A. Rabinovitch, and R. Thieberger, J. Theor. Biol. **160**, 179 (1993).
[27] A. Rabinovitch, R. Thieberger, M. Friedman, and S. Goshen, Chaos Solitons Fractals **7**, 1713 (1996).
[28] H. Treutlein and K. Schulten, Eur. Biophys. J. **13**, 355 (1986).
[29] Ch. Kurrer and K. Schulten, Physica D **50**, 311 (1991).
[30] Ch. Kurrer and K. Schulten, Phys. Rev. E **51**, 6213 (1995).
[31] N. Platt, E.A. Spiegel, and C. Tresser, Phys. Rev. Lett. **70**, 279 (1993).
[32] J.F. Heagy, N. Platt, and S.M. Hammel, Phys. Rev. E **49**, 1140 (1994).
[33] H.A. Kramers, Physica (Amsterdam) **7**, 284 (1940).
[34] P.S. Landa and R.L. Stratonovich, Vestn. Mosk. U. **1**, 33 (1962) (in Russian).